



HELMHOLTZ
ZENTRUM FÜR
INFEKTIONSFORSCHUNG

**This is a postprint of an article published in
Hunke, C., Hirsch, T., Eichler, J.
Structure-based synthetic mimicry of discontinuous protein binding sites:
Inhibitors of the interaction of mena EVH1 domain with proline-rich
ligands
(2006) ChemBioChem, 7 (8), pp. 1258-1264.**

Structure-Based Synthetic Mimicry of Discontinuous Protein Binding Sites: Inhibitors of the Interaction of Mena EVH1 Domain with Proline-Rich Ligands

Cornelia Hunke^[a,b], Tatjana Hirsch^[a] and Jutta Eichler*^[a]

^[a]Dr. C. Hunke, T. Hirsch, Dr. J. Eichler

*GBF – German Research Centre for Biotechnology,
Mascheroder Weg 1, 38124 Braunschweig (Germany)*

Phone: +49-531-6181-793, Fax: +49-531-6181-795

E-mail: jei@gbf.de

^[b]Current address: Nanyang Technological University, School of Biological Sciences, Division of Structural & Computational Biology, 60 Nanyang Drive, Singapore 639798

Abstract

The Mena EVH1 domain, a protein-interaction module found in several proteins that are involved in actin-based cell motility, recognizes proline-rich ligand motifs, which are also present in the sequence of the surface protein ActA of *Listeria monocytogenes*. The interaction of ActA with host Mena EVH1 enables the bacterium to actively recruit host actin in order to spread into neighboring cells. Based on the crystal structure of Mena EVH1 in complex with a polyproline peptide ligand, we have generated a range of assembled peptides presenting Mena EVH1 fragments that make up its discontinuous binding site for proline-rich ligands. Some of these peptides were found to inhibit the interaction of Mena EVH1 with the ligand pGolemi. One of them was further characterized at the level of individual amino acid residues, yielding information on the contribution of individual positions of the peptides to the interaction with the ligand, as well as identifying sites for future structure optimization.

Introduction

Specific interactions between proteins and their ligands are the molecular basis of essentially all protein-mediated biological processes. The exploration of these interactions at the molecular and atomic level is an important step towards the modulation of protein function through controlled interference with the underlying binding events. The design and generation of molecules capable of mimicking conformationally defined binding and/or functional sites of natural proteins, represents a promising strategy for the exploration and understanding of protein structure and function. Such proteinmimetics are also useful tools for a range of biomedical applications, including the inhibition of protein-ligand interactions^[1]. The functional and binding sites of proteins are often not localized in continuous stretches of the amino acid sequence, but rather in sequentially distant fragments of the molecule, which are brought into spatial proximity by protein folding^[2]. Using currently available peptide synthesis strategies, sequentially continuous protein binding sites can be readily mapped, characterized, optimized, and used as lead compounds for inhibitors of protein-ligand interactions. The mimicry of sequentially discontinuous protein binding sites, on the other hand, continues to present a challenge for peptide and organic chemists. Synthetic molecules designed to mimic such discontinuous protein binding sites should present the binding site fragments in a spatial arrangement as similar as possible to the protein structure^[3]. Strategies for the generation of such synthetic mimetics have recently been introduced^[4-8], and used to generate synthetic mimetics of discontinuous protein binding sites of diverse proteins, including the envelope protein of the foot-and-mouth-disease virus^[9] and interleukin-10^[10], as well as the β subunit of follicle stimulating hormone (FSH)^[11].

The actin-based cytoskeleton is the primary mediator of dynamic cellular processes, such as cell motility, focal adhesion, and change of shape^[12,13]. It is regulated by a range of adapter proteins, including the 65 kDa protein mammalian Enabled (Mena), which belongs to the Ena/VASP family of proteins. Mena contains a 112 amino acids long N-terminal EVH1 domain (Mena EVH1), which recognizes proline-rich peptide ligands^[14,15]. This motif is found in several proteins involved in transmitting external signals to the actin cytoskeleton, including the focal adhesion proteins zyxin and vinculin^[16]. Peptide ligands for Mena EVH1 containing the polyproline motif were also identified through synthetic peptide scanning of the bacterial surface protein ActA of the food-borne pathogen *Listeria monocytogenes*^[16,17]. The interaction of ActA with Mena EVH1 of the host cell is the molecular basis for the ability of the bacterium to utilize the actin cytoskeleton to move and infect neighboring cells.

Inhibition of this interaction may therefore provide a strategy to inhibit the motility of the bacterium and, consequently, prevent spreading of the pathogen in the host organism^[15,16,18]. EVH1 domains of Mena^[19], as well as EVL^[20], have been co-crystallized with the peptides FPPPP and EEFPPPT, respectively, which represent the core motif of proline-rich EVH1 ligands (Figure 1). Based on the x-ray crystal structures of these complexes, as well as site-directed mutagenesis studies^[16,21], the binding site and contact residues of Mena EVH1 for the peptide ligand could be identified. The proline-rich core of the ligand forms a PPII helix, which fits into a concave, V-shaped aromatic triad consisting of amino acid residues Y16, W23, and F77 of Mena EVH1. The N-terminal phenylalanine residue of the ligand is also essential for the interaction with Mena EVH1, since its substitution with non-aromatic amino acids largely reduces the affinity to Mena EVH1^[16]. This residue packs into a pocket adjacent to the aromatic triad of Mena EVH1. In ActA, the poly-proline motifs are flanked by clusters of acidic amino acids, which are likely to interact with basic residues in the vicinity of the aromatic triad of Mena EVH1^[18,22]. This notion is supported by the far higher affinity to Mena EVH1 of ActA-derived peptide ligands containing these acidic residues (Ac-DFPPPPTDEEL-NH₂, K_D = 5 μM), compared to a truncated ligand (Ac-FPPPPT-NH₂, K_D = 602 μM)^[19].

1MSEQSICQARAAMVYDDANKK^WVPAGGSTGFSRVHIYHHTGNNTFRVVGRIQD-
 HQVWINCAIPKGLKYNQATQT^FHQWRDARQVYGLNFGSKEDANVFASAMMHALEVLN112

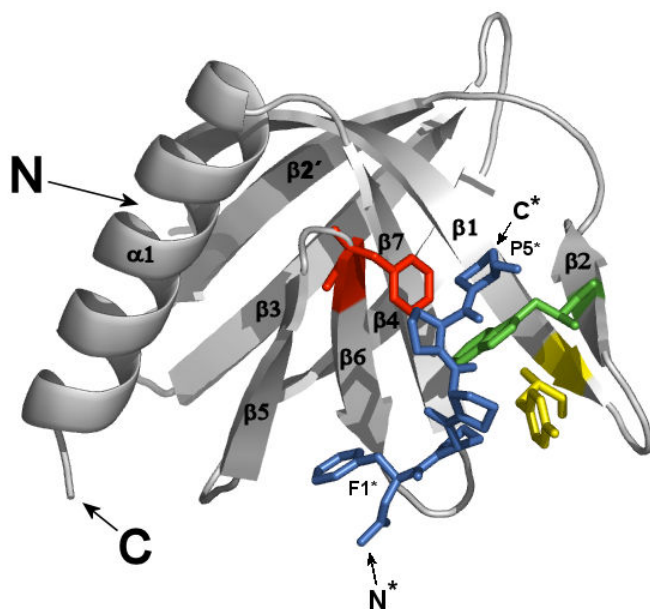


Figure 1. Amino acid sequence of Mena EVH1, and x-ray crystal structure^[19] of Mena EVH1 in complex with the proline-rich ligand FPPPP (blue). The residues making up the aromatic triad of Mena EVH1 are highlighted in yellow (Y16), green (W23) and red (F77), respectively. Ligand positions are denoted with an asterix.

Here we report on the design and generation of synthetic assembled peptides mimicking the sequentially discontinuous binding site of Mena EVH1 for proline-rich ligands, as well as their affinities to a Mena EVH1 ligand.

Results and Discussion

The Mena EVH1 fragments for the design of binding site mimetics, i.e. Fragment A (13VMVYDDANKKVVPA26), and Fragment B (70YNQATQTFHQWR81), were chosen such that they present the residues making up the aromatic triad (Y16, W23, and F77), as well as adjacent basic residues engaged in ionic interactions with acidic residues flanking the polyproline motif in the ligand sequence. Both fragments have loop structures in the crystal structure of the Mena EVH1 – FPPPP complex^[19], presenting two (Fragment A) and one (Fragment B) strands, respectively, of a seven-stranded β -sheet. Furthermore, the N- and C-terminal residues of both fragments are in close proximity (Distances: V13-A26: 6.4 Å, Y70-R81: 8.2 Å). Therefore, both fragments were synthesized as linear, as well as cyclic peptides. A cysteine residue added to the sequence of Fragment A served as ligation point for the reaction with Fragment B, which was equipped with a bromoacetyl moiety as the point of ligation. Both ligation points were introduced either at the N-terminal or C-terminal end of the fragment sequences, enabling variation of fragment orientation within assembled peptides. Furthermore, spacer amino acids with different backbone length, i.e. ϵ -aminohexanoic acid (Ahx), as well as lysine and α,β -diaminopropionic acid (Dap), were inserted between the fragment sequences and the ligation points in order to enable variation of the distance between the two fragments in assembled peptides. When lysine or Dap were used as spacer amino acids, their ϵ - and β -amino groups, respectively, served as attachment sites for the bromoacetyl moiety in Fragment B. Six different peptides presenting Fragment A (**A1-A6**), as well as five peptides presenting Fragment B (**B1-B5**) (Table 1) were synthesized by solid-phase synthesis^[23], and characterized by analytical HPLC with online ESI-MS detection (HPLC-MS).

Table 1. Sequences of peptides presenting Fragment A and Fragment B, as precursors for assembled peptides.

Peptide	Sequence
A1	Ac-Cys-VMVYDDANKKVVPA-NH ₂
A2	Ac-Cys-Ahx ^[a] -VMVYDDANKKVVPA-NH ₂
A3	Ac-VMVYDDANKKVVPA-Cys-NH ₂
A4	Ac-VMVYDDANKKVVPA-Ahx-Cys-NH ₂
A5	cyclo[VMVYDDANKKVVPA-Glu]-Cys-NH ₂
A6	cyclo[VMVYDDANKKVVPA-Glu]-Ahx-Cys-NH ₂
B1	BrAc ^[b] -YNQATQTFHQWR-NH ₂
B2	BrAc-Ahx-YNQATQTFHQWR-NH ₂
B3	Ac-YNQATQTFHQWR-Lys(BrAc)-NH ₂
B4	Ac-YNQATQTFHQWR-Glu]-Dap ^[c] (BrAc)-NH ₂
B5	cyclo[YNQATQTFHQWR-Glu]-Lys(BrAc)-NH ₂

^[a]Ahx, ϵ -aminohexanoic acid; ^[b]BrAc, bromoacetyl; ^[c]Dap, α,β -diaminopropionic acid.

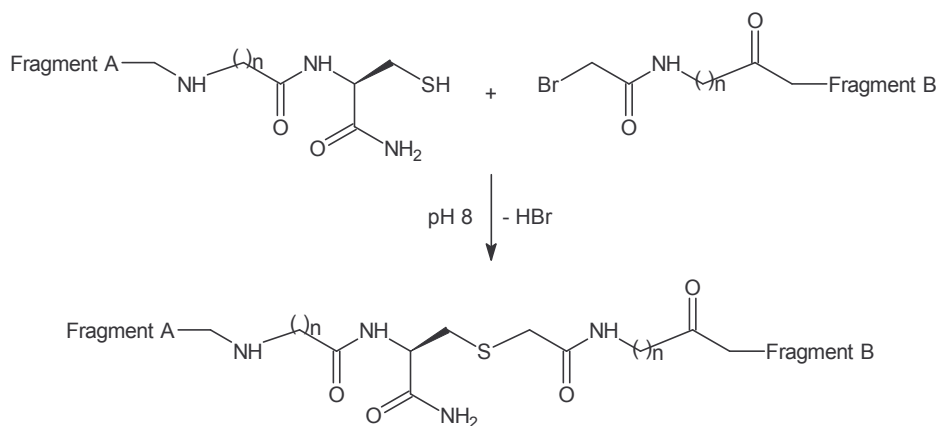


Figure 2. Generation of assembled peptides through thioether formation *via* nucleophilic attack of the SH group of the cysteine residue attached to Fragment A, on the α -carbon of the bromoacetyl group attached to Fragment B.

Assembled peptides were generated through reaction of the sulfhydryl group of the cysteine residue attached to Fragment A, with the bromoacetyl moiety attached to Fragment B, generating a thioether bridge between the two fragments (Figures 2 and 3). This chemo-selective ligation reaction proceeds in aqueous buffer solutions at pH 8-9^[24]. A total of 30 (6 \times 5) assembled peptides (**P1-P30**, Table 2) were generated by linking each Fragment A precursor to each Fragment B precursor in a combinatorial fashion, and the resulting ligation products used directly in subsequent binding assays.

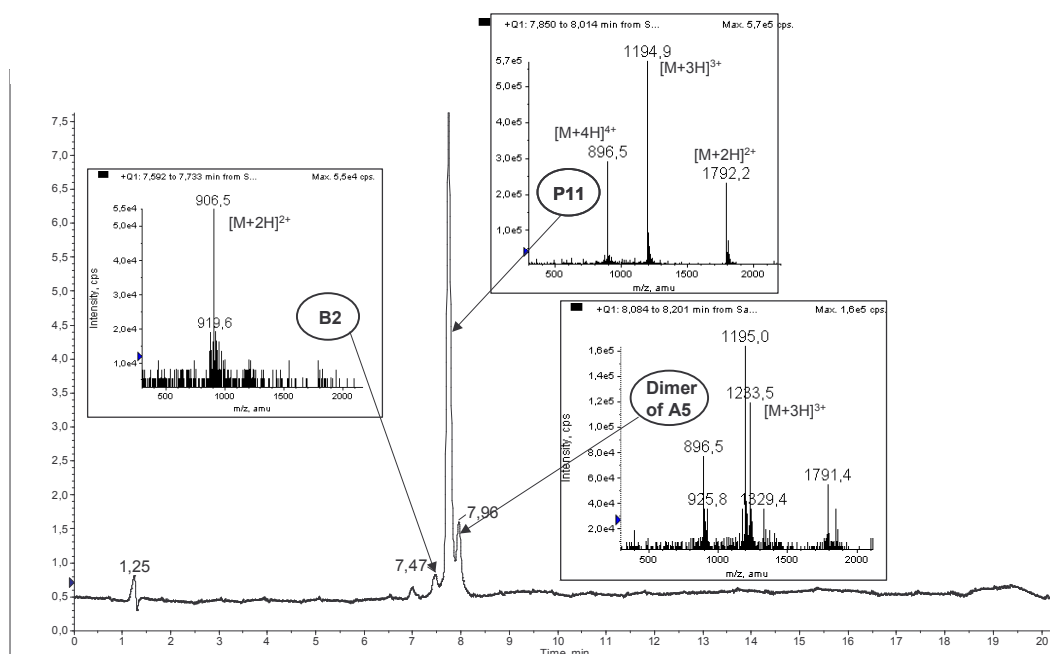


Figure 3. HPLC chromatogram and ESI mass spectra of **P11**, containing as the main product the correct assembled peptide ($M = 3582$), as well as unreacted **B2** ($M = 1812$) and the dimer of **A5** ($M = 3696$), as minor impurities.

Table 2. Precursor combinations used to generate assembled peptides, their molecular weights and ESI mass spectrometry data (rounded to whole numbers).

Peptide	Precursor Combination	M (calc.)	M (mass spec)	Peptide	Precursor Combination	M (calc.)	M (mass spec)
P1	A1 + B1	3399	1701 [M+2H] ²⁺	P16	A4 + B3	3682	1844 [M+2H] ²⁺
			1134 [M+3H] ³⁺				1228 [M+3H] ³⁺
P2	A2 + B1	3512	1757 [M+2H] ²⁺	P17	A5 + B3	3639	1214 [M+3H] ³⁺
			1172 [M+3H] ³⁺				
P3	A3 + B1	3399	1701 [M+2H] ²⁺	P18	A6 + B3	3752	1252 [M+3H] ³⁺
			1134 [M+3H] ³⁺				939 [M+4H] ⁴⁺
P4	A4 + B1	3512	1172 [M+3H] ³⁺	P19	A1 + B4	3527	1177 [M+3H] ³⁺
			879 [M+4H] ⁴⁺				883 [M+4H] ⁴⁺
P5	A5 + B1	3469	1735 [M+2H] ²⁺	P20	A2 + B4	3640	1214 [M+3H] ³⁺
			1157 [M+3H] ³⁺				911 [M+4H] ⁴⁺
P6	A6 + B1	3582	1195 [M+3H] ³⁺	P21	A3 + B4	3527	1177 [M+3H] ³⁺
			896 [M+4H] ⁴⁺				883 [M+4H] ⁴⁺
P7	A1 + B2	3512	1172 [M+3H] ³⁺	P22	A4 + B4	3640	1214 [M+3H] ³⁺
			879 [M+4H] ⁴⁺				911 [M+4H] ⁴⁺
P8	A2 + B2	3625	1209 [M+3H] ³⁺	P23	A5 + B4	3597	1200 [M+3H] ³⁺
			907 [M+4H] ⁴⁺				900 [M+4H] ⁴⁺
P9	A3 + B2	3512	1171 [M+3H] ³⁺	P24	A6 + B4	3710	1237 [M+3H] ³⁺
			879 [M+4H] ⁴⁺				928 [M+4H] ⁴⁺
P10	A4 + B2	3625	1209 [M+3H] ³⁺	P25	A1 + B5	3639	n.d.
			907 [M+4H] ⁴⁺				
P11	A5 + B2	3582	1195 [M+3H] ³⁺	P26	A2 + B5	3752	1252 [M+3H] ³⁺
			896 [M+4H] ⁴⁺				939 [M+4H] ⁴⁺
P12	A6 + B2	3695	1233 [M+3H] ³⁺	P27	A3 + B5	3639	1214 [M+3H] ³⁺
			925 [M+4H] ⁴⁺				911 [M+4H] ⁴⁺
P13	A1 + B3	3569	1191 [M+3H] ³⁺	P28	A4 + B5	3752	1252 [M+3H] ³⁺
			893 [M+4H] ⁴⁺				939 [M+4H] ⁴⁺
P14	A2 + B3	3682	1228 [M+3H] ³⁺	P29	A5 + B5	3710	1237 [M+3H] ³⁺
			922 [M+4H] ⁴⁺				928 [M+4H] ⁴⁺
P15	A3 + B3	3569	1191 [M+3H] ³⁺	P30	A6 + B5	3823	n.d.
			893 [M+4H] ⁴⁺				

In order to evaluate the Mena EVH1- mimicking character of the assembled peptides, they were tested for their ability to inhibit the Mena EVH1 – ligand interaction. We have established a competitive Mena EVH1 binding assay in microtiter plates using plate-bound recombinant GST-Mena EVH1^[25] in conjunction with the engineered Mena-EVH1 ligand pGolemi^[26], which was synthesized by solid-phase synthesis, and N-terminally biotinylated for detection (Biotin-PFPPTPPGEEAPVEDLIRFYNDLQQYLNVV-NH₂). The readout of this assay is inhibition of binding of Biotin-pGolemi to plate-bound GST-Mena EVH1, by the Mena EVH1 – derived assembled peptides. The inhibitory effects of assembled peptides were compared using IC₅₀ values (Table 3, Figures 4 and 5) as a ranking parameter.

Table 3. IC₅₀ values of assembled peptides in the competitive GST-Mena EVH1 – pGolemi binding assay.

Assembled Peptide	IC ₅₀ [μM]	Assembled Peptide	IC ₅₀ [μM]	Assembled Peptide	IC ₅₀ [μM]
P1	32	P11	5	P21	50
P2	26	P12	8	P22	> 140
P3	24	P13	33	P23	31
P4	20	P14	12	P24	> 140
P5	15	P15	> 140	P25	> 140
P6	17	P16	> 140	P26	> 140
P7	24	P17	33	P27	> 140
P8	14	P18	> 140	P28	71
P9	21	P19	62	P29	> 140
P10	32	P20	69	P30	> 140
Mena-EVH1	0.189				

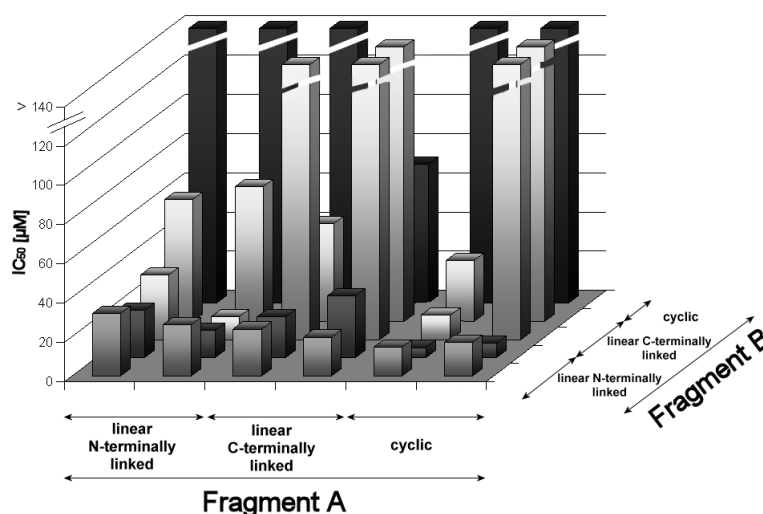


Figure 4. Influence of orientation and conformational constraint of Fragments A and B on the affinity of assembled peptides to pGolemi.

For Fragment A, orientation within the assembled peptides (N- vs. C-terminal linkage to Fragment B), as well as conformational constraint through cyclization, are of limited relevance for the inhibitory activity, since the variation of these parameters does not significantly alter the IC₅₀ values of assembled peptides. Fragment B, on the other hand, is preferably linked to Fragment A as a linear peptide *via* its N-terminus, since the IC₅₀ values of most of the peptides containing a C-terminally linked and/or cyclic Fragment B (P13-P30) are

significantly higher than those containing an N-terminally linked, linear Fragment B (**P1-P12**). Furthermore, the distance between the two fragments appears to be less important for the affinity of assembled peptides to pGolemi, since peptides differing only in the spacer amino acids (e.g. **P1** and **P2**, as well as **P11** and **P12**), have similar IC_{50} values. This fact may imply that even the peptides with the shortest distance between the two fragments are sufficiently flexible to assume conformations required for binding to the ligand.

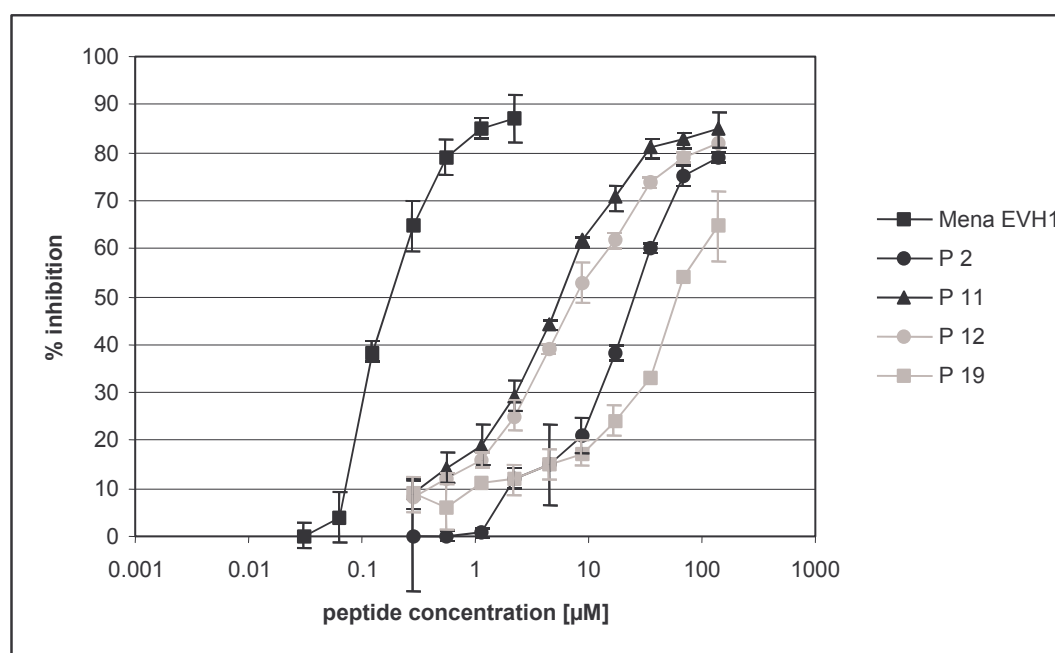


Figure 5. Inhibition of the GST-Mena EVH1 – pGolemi interaction by Mena EVH1 and assembled peptides.

The strongest inhibition of the interaction of Mena EVH1 with pGolemi was found for **P11** and **P12** (IC_{50} values: 5 and 8 μ M, respectively, Figure 5), in which cyclic Fragment A is linked to the N-terminus of linear Fragment B *via* one and two ϵ -aminohexanoic acid (Ahx) spacers, respectively (Figure 6). After purification by preparative HPLC, the inhibitory activity of **P11** ($IC_{50} = 11 \mu$ M) was approximately 60 times lower than that of Mena EVH1 itself ($IC_{50} = 189$ nM). Peptides representing only one of the fragments used to generate **P11** and **P12** (*cyclo*[VMVYDDANKKWPVPA-Glu]-Ahx-A-NH₂, $IC_{50} = 130 \mu$ M, and Ac-Ahx-YNQATQTFHQWR-NH₂, $IC_{50} = 190 \mu$ M) had 20 to 30 times lower affinities than **P11** and **P12**, indicating a synergistic effect of combining both fragments in one molecule. **P11** was also tested also for its ability to inhibit the interaction of plate-bound GST-Mena EVH1 with the natural peptide ligand ActA₁₁ (DFPPPPTDEEL), derived from the surface protein ActA of *L. monocytogenes*^[16], whose affinity to Mena EVH1 had been shown to be 10-fold lower than that of pGolemi^[26]. Consequently, ActA₁₁ was used in the binding assay at a 10-fold higher concentration than pGolemi (1 μ M vs. 0.1 μ M). As pGolemi, ActA₁₁ was synthesized on solid

phase, and N-terminally biotinylated for detection. The Mena EVH1 – ActA₁₁ interaction was inhibited by **P11** (IC₅₀ = 14.5 μM), demonstrating its ability to mimic the binding behaviour of Mena EVH1 also in the interaction with a native proline-rich ligand.

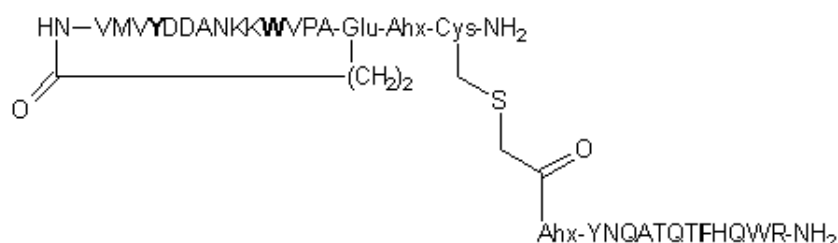


Figure 6. Chemical structure of **P12**, presenting cyclic Fragment A and linear Fragment B. The Ahx residue between Fragment A and the cysteine residue is omitted in **P11**.

By testing direct binding of biotinylated pGolemi and GST-Mena-EVH1, respectively, to plate-bound **P11**, it could be shown that the assembled peptides inhibit the Mena-EVH1 – pGolemi interaction by binding to pGolemi, and not to GST-Mena-EVH1 (Figure 7).

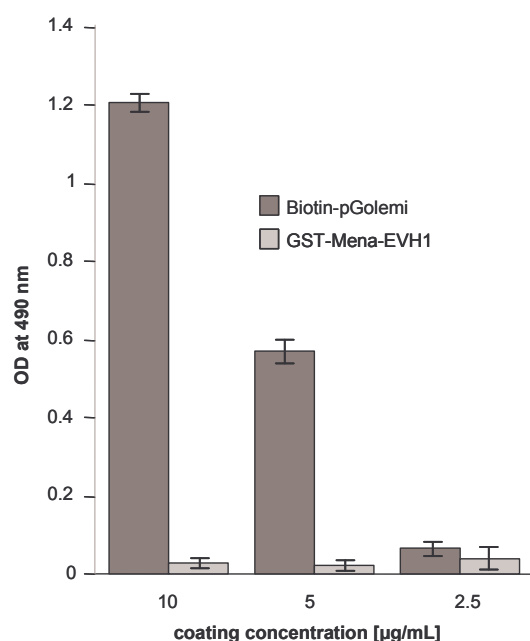


Figure 7. Direct binding of Biotin-pGolemi (0.1 μM) and GST-Mena-EVH1 (3 μg/mL) **P11** adsorbed to a Microtest plate (Sarstedt). Detection: anti-Biotin-HRP and anti-GST-HRP, respectively.

In order to evaluate the binding specificities of the assembled peptides as a criteria for their Mena EVH1 mimicking character, an analog of **P12** was synthesized and tested, in which all three residues representing the aromatic triad of Mena EVH1 were replaced by alanine. For the generation of this analog, two new precursor fragments (*cyclo*[VMVADDANKKAVPA-Glu]-Ahx-Cys-NH₂ and BrAc-Ahx-YNQATQTAHQWR-NH₂) were synthesized. The resulting assembled peptide did not inhibit the Mena EVH1 -

pGolemi interaction ($IC_{50} > 300 \mu\text{M}$), indicating a related mode of binding to proline-rich ligands for Mena EVH1 and the assembled peptides mimicking its binding site. Likewise, the inhibitory activity of a scrambled assembled peptide containing the same amino acid residues as **P11**, but in mixed-up sequences, which was generated through ligation of the scrambled precursor peptides *cyclo*[KPVAWMADVVDNYK-Glu]-Cys-NH₂ and BrAc-Ahx-QRHYTWNTQAQF-NH₂, was largely decreased ($IC_{50} > 62 \mu\text{M}$), providing further evidence for a sequence-specific interaction of the Mena EVH1 mimetic peptides with pGolemi.

The interaction of **P12** with pGolemi was further examined, at the level of individual amino acid residues, using 24 new assembled peptides, in which all positions, except positions 19 and 73 of Mena EVH1, which are occupied with alanine in **P12**, were successively replaced by alanine. Peptides representing the complete Ala-scan of **A6** und **B2**, respectively, were synthesized as precursors, ligated to the respective unmodified complementary fragment, and the resulting assembled peptides tested in the competitive Mena EVH1 binding assay (Figure 8). Substitution of most positions of **P12** with alanine resulted in significant loss of affinity to pGolemi, as demonstrated by the generally higher IC_{50} values compared to the **P12**, implying a substantial contribution of many positions within **P12** to the interaction with the ligand. As expected, this effect was strongly pronounced for the three residues making up the aromatic triad, i.e. Y16, ($IC_{50} = 85 \mu\text{M}$), W23 ($IC_{50} = 124 \mu\text{M}$) and F77 ($IC_{50} = 222 \mu\text{M}$), however, the variation of IC_{50} values among the three peptides points to different individual contributions of the three triad positions to the interaction with the ligand. This question could not be addressed using the previously mentioned assembled analog of **P12**, in which all three triad positions were replaced by alanine at the same time. Apart from the aromatic triad, other, particularly basic residues (K21, R81), are clearly important for the interaction with the ligand (IC_{50} values: $136 \mu\text{M}$ and $81 \mu\text{M}$, respectively), which confirms, at the level of synthetic peptides mimicking the Mena EVH1 binding site, the reported stabilization of the interaction of the Mena EVH1 – ligand complex through ionic interactions between acidic residues flanking the polyproline motif of the ligand, and basic residues in the vicinity of the aromatic triad of Mena EVH1^[19,22]. Only two positions of **P12** (D18 and N20) were shown to be largely insensitive to replacement with alanine ($IC_{50} < 10 \mu\text{M}$), and the substitution of two more positions (Q72 and W80) had only a weak effect on the affinity to pGolemi ($IC_{50} < 20 \mu\text{M}$). These positions can serve as target points for structure optimization of assembled peptides through systematic replacement with other proteinogenic

and non-proteinogenic amino acids, with the aim to improve the affinity of synthetic Mena EVH1 binding site mimetics to proline-rich ligands.

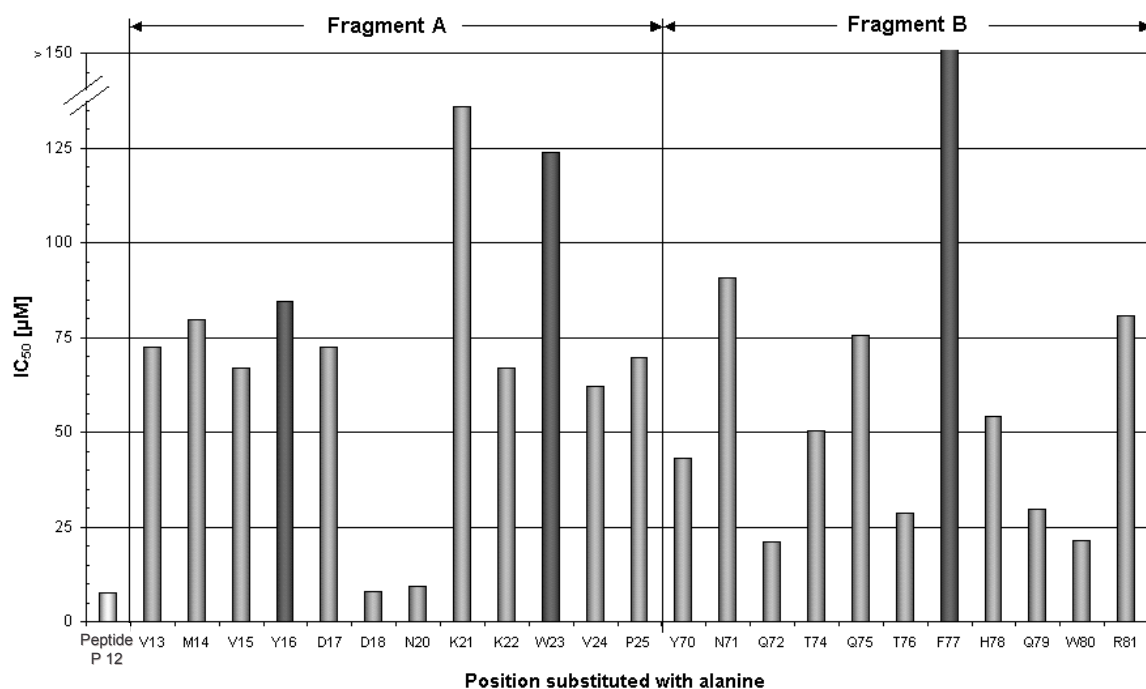


Figure 8. Affinity to pGolemi of assembled peptides representing the complete Ala-scan of **P12**. Numbering of positions was kept in accordance with Mena EVH1. Bars in darker shade represent peptides, in which one of the three aromatic triad positions was replaced with alanine.

In conclusion, the concept of structure-based synthetic mimicry of discontinuous protein binding sites through assembled peptides presenting sequentially distant protein fragments in one molecule, has been successfully used to design and generate synthetic mimetics of the Mena EVH1 binding site for proline-rich ligands. These peptides inhibit the interaction of Mena EVH1 with pGolemi, and their mode of binding is closely related to that of Mena EVH1. Such binding site mimetics present a starting point for the development, through systematic structure optimization, of inhibitors of the interaction of ActA of *L. monocytogenes* with host cell Mena EVH1.

Experimental Section

Protein production. Mena EVH1 domain was produced as an N-terminal glutathione S-transferase (GST) fusion protein in *E. coli* strain BL21(DE3) Codon Plus from Stratagene. Cells were cultured at 37°C in LB medium containing 100 µg/mL ampicillin, to an OD of 0.7-0.9 at 600 nm. Prior to induction with isopropylthio-D-galactoside (final concentration: 0.1 mM), cells were cooled to 20 °C. Cell culturing was continued for 20 h. After French press cell lysis and centrifugation, the supernatant was applied to a glutathione-Sephadex column

from Pharmacia. GST-Mena EVH1 was eluted with 10 mM reduced glutathione in Tris buffer pH 8.0, and concentrated using a 15 mL concentrator (Centricon from Vivascience). The protein was further purified by gel filtration on a HiLoad Superdex 16/60 column from Amersham using HEPES buffer as eluent. The purified protein was concentrated to 2.2 mg/mL, and 40 μ L-aliquots of this solution in phosphate buffer containing 1mM 1,4-dithiothreitol and 4 mM protease inhibitor cocktail (Complete from Roche), were shock-frozen in liquid nitrogen, and stored at -70°C.

Peptide synthesis. Peptide fragments as precursors for assembled peptides, as well as N-terminally biotinylated pGolemi and ActA₁₁, were synthesized as C-terminal amides by Fmoc-based solid-phase peptide synthesis on TentaGel S RAM (0.25 mmol/g), using the automated parallel peptide synthesizer SYRO from MultiSynTech. In a standard coupling cycle, five eq. of Fmoc-amino acid/DIC/HOBt in DMF were coupled for 60 min. In peptides presenting Fragment B, bromoacetic acid (10 eq.) was coupled for 1 hour, after pre-activation with DIC, either to the N-terminal amino group, or, after removal of the ivDde group using a solution of 2% hydrazine hydrate and 10% allylic alcohol in DMF (8 x 7 min.), to the side chain of the C-terminal Lys and Dap residues, respectively. In cyclic peptides, a side chain allyl-protected Glu residue was added C-terminally to the fragment sequence. The allyl ester was cleaved by treating the resin overnight with a solution of Pd(PPh₃)₄, (8.6 mg/mL) and 1,3-dimethylbarbituric acid (13 mg/mL) in DMF/THF 5 : 2 under argon. Peptides were cyclized on the resin through amide formation between the N-terminal amino group and the γ -carboxy group of the C-terminal Glu residue (5 eq. PyBOP/HOBt, 10 eq. DIEA, overnight). Peptides were cleaved from the resin using a mixture of TFA/DCM/triisopropylsilane/water (70:20:5:5) for 2 hours, precipitated in a cold 1:1 mixture of cyclohexane and *tert*-butyl methyl ether, extracted with water, and lyophilized twice. Cleaved peptides were analyzed by analytical HPLC (Column: PLRP-S 100 Å, 3 μ m, 50 x 2.1 mm, flow rate: 0.4 mL/min, gradient: 5-65% acetonitrile in H₂O, both containing 0.05% TFA, in 15 min) with online ESI-MS detection (HPLC-MS), and purified by preparative HPLC (Column: Nucleosil RP18, 250 x 10 mm, flow rate: 3 mL/min, gradient: 5-65% acetonitrile in H₂O, both containing 0.1% TFA, in 60 min, UV detection: 220 nm).

Generation of assembled peptides. The peptide precursor solutions (50 μ L, 2.5 mM in 50% acetonitrile/water) were mixed and reacted overnight after addition of 100 μ L phosphate buffer pH 9.2. Completeness of the reaction was confirmed by a negative Ellman test^[27].

Formation of the assembled peptide was confirmed by analytical HPLC-MS, and the solutions used directly, without further purification, in the binding assays. **P11** was further purified by preparative HPLC (for conditions, see Section *Peptide Synthesis* above).

Competitive Binding assay. The wells of 96-well sulfhydryl binding microtiter plates (Corning) were coated for 1 hour with 100 μ L GST-Mena EVH1 (0.1 μ g/mL in phosphate buffer pH 7.2). Unspecific binding was blocked by treating the plate for three hours with phosphate buffer pH 7.2, containing 1% BSA and 0.01% Tween. The plate was then incubated overnight at 4°C with 50 μ L peptide solution at various concentrations (serial two-fold dilutions), and 50 μ L 0.1 μ M Biotin-pGolemi, or 50 μ L 1 μ M Biotin-Ahx-ActA₁₁ (all solutions in phosphate buffer containing 0.1% BSA and 0.01% Tween) . Bound ligand was detected using an anti-Biotin-HRP conjugate (1 hour, dilution: 1:2000 in phosphate buffer pH 7.2, containing 0.1% BSA and 0.01% Tween), followed by developing the plates in the dark with 100 μ L OPD solution (1 mg/mL in 0.03% H₂O₂/water). The reaction was stopped after approximately 15 minutes by adding 50 μ L 4 N sulfuric acid, and absorbances (ODs) were read at 490 nm using a multichannel photometer (Spectramax 250). IC₅₀ values were calculated, using the program SigmaPlot, from inhibition values at different peptide concentrations (average of duplicate data points), which were determined according to the following formula:

$$\% \text{ Inhibition} = [1 - (\text{OD}_{\text{sample}} - \text{OD}_{\text{blank}}) / (\text{OD}_{\text{control}} - \text{OD}_{\text{blank}})] \times 100,$$

in which “control” is a sample without peptide, and "blank" is a sample without peptide and without coated GST-Mena EVH1.

Acknowledgements

This work was funded by the BioFuture Program (Grant # 0311882) of the German Federal Department of Education and Research (BMBF). We thank Dirk Heinz for providing the GST-Mena EVH1 expressing *E. coli* strain and Mena EVH1, Theresia Stradal for GST-Mena EVH1, and Heike Overwin for technical assistance.

Key words

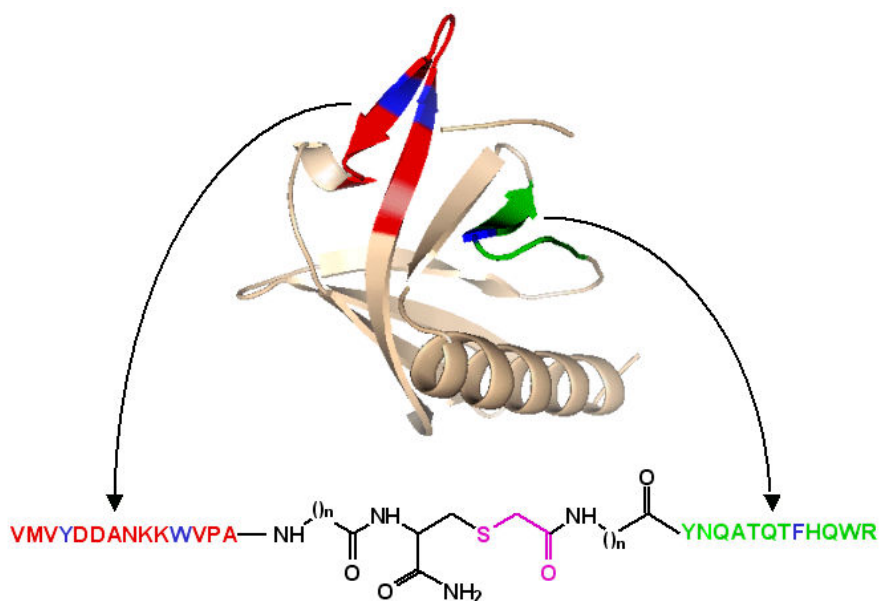
Protein-ligand interactions, peptide, biomimetic synthesis, structure-based design, EVH1 domain.

References

- [1] J. Eichler, *Comb.Chem.High T.Scr.* **2005**, *8*, 135-143.
- [2] D.J. Barlow, M.S. Edwards, J.M. Thornton, *Nature* **1986**, *322*, 747-748.
- [3] J. Eichler, *Protein Peptide Lett.* **2004**, *11*, 281-290.
- [4] R. Franke, C. Doll, V. Wray, J. Eichler, *Protein Peptide Lett.* **2003**, *10*, 531-539.
- [5] R. Franke, C. Doll, V. Wray, J. Eichler, *Org.Biomol.Chem.* **2004**, *2*, 2847-2851.
- [6] P. Timmermann, J. Beld, W.C. Pujik, R.H. Meloen, *Chembiochem.* **2005**, *6*, 821-824.
- [7] T. Opatz, R.M. Liskamp, *Org.Lett.* **2001**, *3*, 3499-502.
- [8] F. Peri, D. Grell, P. Dumy, Y. Yokokawa, K. Welzenbach, G. Weitz-Schmidt, M. Mutter, *J.Pept.Sci.* **1999**, *5*, 313-22.
- [9] J. Villen, E. Borrás, W.M. Schaaper, R.H. Meloen, M. Davila, E. Domingo, E. Giralt, D. Andreu, *Chembiochem.* **2002**, *3*, 175-82.
- [10] U. Reineke, R. Sabat, R. Misselwitz, H. Welfle, H.D. Volk, J. Schneider-Mergener, *Nat.Biotechnol.* **1999**, *17*, 271-275.
- [11] P. Timmerman, E. Van Dijk, W. Puijk, W. Schaaper, J. Sloostra, S.J. Carlisle, J. Coley, S. Eida, M. Gani, T. Hunt, P. Perry, G. Piron, R.H. Meloen. *Mol.Div.* **2004**, *8*, 61-70.
- [12] T.J. Mitchison, L.P. Cramer, *Cell* **1996**, *84*, 371-379.
- [13] M.F. Carlier, C. Le Clainche, S. Wiesner, D. Pantaloni, *Bioessays* **2003**, *25*, 336-345.
- [14] L.J. Ball, T. Jarchau, H. Oschkinat, U. Walter, *FEBS Letters* **2002**, *513*, 45-52.
- [15] F.B. Gertler, K. Niebuhr, M. Reinhard, J. Wehland, P. Soriano, *Cell* **1996**, *87*, 227-239.
- [16] K. Niebuhr, F. Ebel, R. Frank, M. Reinhard, E. Domann, U.D. Carl, U. Walter, F.B. Gertler, J. Wehland, T. Chakraborty, *EMBO J.* **1997**, *16*, 5433-5444.
- [17] L.J. Ball, R. Kuehne, B. Hoffmann, A. Haefner, P. Schmieder, R. Volkmer-Engert, M. Hof, M. Wahl, J. Schneider-Mergener, U. Walter, H. Oschkinat, T. Jarchau, *EMBO J.* **2000**, *19*, 4903-4914.
- [18] G.A. Smith, J.A. Theriot, D.A. Portnoy, *J.Cell Biol.* **1996**, *135*, 647-660.
- [19] K.E. Prehoda, D.J. Lee, W.A. Lim, *Cell* **1999**, *97*, 471-480.
- [20] A.A. Fedorov, E. Fedorov, F. Gertler, S.C. Almo, *Nat.Struct.Biol.* **1999**, *6*, 661-665.
- [21] L.J. Ball, R. Kuehne, J. Schneider-Mergener, H. Oschkinat, *Angew.Chem.Int.Ed Engl.* **2005**, *44*, 2852-2869.
- [22] U.D. Carl, M. Pollmann, E. Orr, F.B. Gertler, T. Chakraborty, J. Wehland, *Current Biology* **1999**, *9*, 715-718.
- [23] W.C. Chan, P.D. White, *Fmoc solid phase peptide synthesis: A practical approach*, Oxford University Press, Oxford, **2000**.
- [24] (a) D.R. Englebretsen, C.T. Choma, G.T. Robillard. *Tet.Lett.* **1998**, *39*, 4929-4932. (b) J.A. Wilce, S.G. Love, S.J. Richardson, P.F. Alewood, D.J. Craik, *J.Biol.Chem.* **2001**, *276*, 25997-26003. (c) D.R. Englebretsen, B. Garnham, P.F. Alewood. *J.Org.Chem.* **2002**, *67*, 5883-5890.

- [25] M.P. Machner, C. Urbanke, M. Barzik, S. Otten, A.S. Sechi, J. Wehland, D.W. Heinz, D.W. *J.Biol.Chem.* **2001**, *276*, 40096-40103.
- [26] D. Golemi-Kotra, R. Mahaffy, M.J. Footer, J.H. Holtzmann, T.D. Pollard, J.A. Theriot, A. Schepartz, *J.Am.Chem.Soc.* **2004**, *126*, 4-5.
- [27] Ellman, G.L. *Arch.Biochem.Biophys.* **1959**, *82*, 70-77.

Graphical Abstract



Text for Table of Contents

Based on the crystal structure of a complex of the protein interaction domain Mena EVH1 with a proline-rich ligand, assembled peptides presenting two Mena EVH1 fragments, which make up its discontinuous binding site for proline-rich ligands, were generated and tested for their ability to mimic the binding behavior of Mena EVH1.